Electronic Supporting Information for:

A phase-transfer crystallization pathway to synthesize ultrasmall silicoaluminophosphate for enhanced catalytic conversion of dimethylether-to-olefin†

Hongxin Ding[a], Jiajia Ding[b], Wei Liu[b], Xiaoling Zhao[a], Qijin Chi[c], Kake Zhu[a]*, Xinggui Zhou[a], Weimin Yang[b]*

[a]*State Key Laboratory of Chemical Engineering, East China University of Science and Technology, Shanghai 200237, P. R. China.*
[b]*Shanghai Research Institute of Petrochemical Technology, Sinopec, Shanghai 201208, P. R. China.*
[c]*Department of Chemistry, Technical University of Denmark, Kemitorvet Building 207, DK-2800 Kongens Lyngby, Denmark*

Table of contents

A. Materials and methods

Materials: The reagents used were aluminum isopropoxide (AIP, >98 %, TCI), phosphoric acid (85 wt%, Shanghai Lingfeng Chemical Reagent Co. Ltd.), tetraethylammonium hydroxide (TEAOH) (35 wt%, Shanghai Cainorise Chemicals Co., Ltd), tetraethyl orthosilicate (TEOS, 28 wt % SiO_2, Shanghai Lingfeng Chemical Reagent Co. Ltd), toluene (>99.8 wt %, Shanghai Lingfeng Chemical Reagent Co. Ltd).

Synthesis procedure: SAPO-34-N was prepared using a phase-transfer synthesis process. The molar composition ratio of the synthesis gel was 1.0 Al_2O_3: 1.0 P_2O_5: 0.3 SiO_2: 2.0 TEAOH: 50 H_2O: 6.5 toluene. In a typical synthesis, 2.19 g TEOS was mixed with 3.84 g H_3PO_4 and 3.76 g deionized water to form a mixture, to which 14.03 g TEAOH was added dropwise after 2 h stirring. The mixture was further stirred for 4 h and named solution A. In another beaker, 6.81 g AIP was dissolved in 10.00 g toluene by mechanical stirring for 3 h to produce solution B. Solutions A and B were mixed and transferred to a 100 mL Teflon lined stainless steel autoclave for crystallization. Crystallization was conducted at 473 K under tumbling of 50 rpm for 48 h. The product was centrifuged, washed thoroughly with water before drying at 353 K for 6 h, followed by calcination at 823 K for 6 h. To investigate the crystallization, part of the gel was sampled at various crystallization intervals and denoted by using synthesis time as suffix. For example, SAPO-34-N-12h represent the sample was hydrothermally treated for 12h.

Conventional counterpart SAPO-34-C was derived from aqueous static crystallization otherwise identical crystallization conditions as that of SAPO-34-N. A series of controlled experiments SAPO-34-D-W derived from aqueous dynamic crystallization, and SAPO-34-S-W-T prepared from water-toluene biphasic media under static crystallization, SAPO-34-PB-D-W derived from aqueous dynamic crystallization from pseudoboehmite, and SAPO-34-PB-D-W-T prepared from water-toluene biphasic media using pseudoboehmite as precursor under otherwise identical crystallization conditions as that of SAPO-34-N; SAPO-34-W:T=50:3.2& SAPO-34-W:T=50:13 just turn water toluene radio from 50:3.2 to 50:13 under otherwise identical crystallization conditions as that of SAPO-34-N. Detailed synthetic procedures are tabulated in Table S3.

B. Characterization techniques

X-ray diffraction (XRD) patterns were gathered using a Rigaku 2550VB/PC

diffractometer operating at 40 kV and 100 mA with Cu Kα X-ray source (λ = 1.5418 Å).

Scanning electron microscopy (SEM) were captured on NOVA Nano SEM 450 (FEI) and Gemini SEM 500 (Carl Zeiss) and transmission electron microscopy (TEM) were captured on images JEL-2011 (JEOL) instruments.

N_2 physisorption measurements were conducted on an ASAP 2020 HD (Micromeritics, USA) analyzer at 77 K, all samples were degassed at 623 K for 24 h under vacuum before measurements. The surface areas were determined by the Brunauer-Emmett-Teller (BET) method. Micropore volumes and surfaces were derived from a *t*-plot approach, pore size distribution was derived from adsorption branch using Barret-Joyner-Halenda (BJH) method, and the total pore volume values were estimated by the adsorption at a relative pressure $p/p_0 = 0.99$.

Ammonium temperature programed desorption (NH_3-TPD) measurements were performed on an AutoChem II (Micromeritics, USA) analyzer. The samples were pretreated at 873 K for 1 h under He flow before saturated with ammonium at 373 K. The profiles collected between 373 K and 873 K at a ramp of 10 $K \cdot min^{-1}$.

Elementary compositions were measured by inductively coupled plasma optical emission spectrometry (ICP) on an IRIS 1000 instrument.

Dynamic Light Scattering (DLS) measurements were performed on NICOMP 380 ZLS instrument.

^{29}Si, ^{27}Al and ^{31}P solid state magic angle spinning nuclear magnetic resonance (MAS NMR) measurements were obtained on a Varian 400 spectrometer, 4 mm ZrO_2 rotors with a spinning rate of 8-10 kHz at room temperature. ^{27}Al MAS NMR spectra were recorded at a resonance frequency of 104.26 MHz. ^{27}Al chemical shifts were reported relative to 0.1 M aqueous $Al(NO_3)_3$ solution. ^{29}Si and ^{31}P MAS NMR measurements were performed at a resonance frequency of 79.49 MHz and 161.98MHz, respectively. The ppm scale was referenced to $Si(CH_3)_4$ for ^{29}Si and $(NH_4)H_2PO_4$ for ^{31}P.

FT-IR spectra were obtained with a Nicolet 6700 instrument. 1 mg sample was mixed with 99 mg KBr powder to prepare self-support pellets used for FT-IR measurement.

Diffuse reflectance infrared Fourier-transform spectra (DRIFTS) were recorded using a Nicolet 380 spectrometer at 4 cm^{-1} resolutions. Prior to measurement, catalysts were first activated at 674 K under vacuum for 2h. The background spectrum recorded under identical operating conditions except in the absence of a sample in the

cell, was always automatically subtracted from measured spectra.

Gas chromatography-mass spectrometry (GC-MS) were performed on a Agilent 7890B GC/5977B, equipped with MSD&CTC Analytics, 2 mL sample was headspace injected after 363 K for 30 min.

C. Diffusivity measurements

The diffusivity of propylene in the SAPO-34 samples was measured by gravimetric analysis, using an Intelligent Gravimetric Analyzer, model IGA-100, from Hiden Analytical Ltd., Warrington, UK. The system consists of a fully computerized microbalance, which automatically measures the weight of the sample sorbents as a function of time with the gas vapor pressure and sample temperature under computer control. The sensitivity of the microbalance was 1 μg. The calcined sample (0.10 g) was pretreated at a pressure of $< 10^{-6}$ Pa and 573 K in a N_2 atmosphere for 3 h to remove adsorbed impurities until the sample held a constant weight. Afterwards, the sample was cooled to 365 K and the contacting gas was replaced by a preset amount of gaseous mixture, consisting of propylene and N_2 (N_2 saturated with propylene at 323 K, 100 mL/min). Isotherms and the corresponding kinetics of adsorption and desorption were determined at varied partial pressure (P/P_0 = 0-1) steps.

To quantify to which extent diffusion resistance was mitigated by reduction of crystal size, diffusion measurements were carried out with propylene as a representative adsorbate. The effective diffusivity was estimated using Fick's second law, which expresses the concentration variation of molecules inside a porous slab (assumed infinitely extended in the transverse direction) as a function of exposure time:

$$\frac{\partial C}{\partial t} = D_{eff}\left(\frac{\partial^2 C}{\partial x^2}\right) \tag{1}$$

where C is the concentration of propylene inside the particle, t is time, D_{eff} is the diffusivity, and x is the distance, measured from the center of a slab.

At the beginning of adsorption process in a slab-like crystal, the solution of this equation can be well approximated

$$\frac{q(t)}{q(\infty)} = \frac{6}{\sqrt{\pi}}\sqrt{\frac{D_{eff}}{L^2}}\sqrt{t} \tag{2}$$

where $q(t)/q(\infty)$ is the normalized hydrocarbon uptake and L is the characteristic diffusion length.

D. Catalytic assessment and carbon deposit analyses

Dimethyl ether to olefin conversion (DTO) was carried out on a fix bed reactor at atmospheric pressure. 100 mg catalyst (60-80 mesh) was preheated at 823 K for 3h under N_2 flow before reaction. Reaction temperature was 723 K and the dimethyl ether weight hourly space velocity (WHSV) was 2 h^{-1}. The products were analyzed by an on-line gas chromatograph equipped with a flame ionization detector (FID) and Plot-Q column (Agilent J&W GC Columns, HP-PLOT/Q 19091P-Q04, 30 m × 320 μm × 20 μm). The conversion and selectivity were calculated on CH_2 basis and methanol was considered as reactant in the calculation.

$$\text{DME conversion} = \frac{1 - (\text{C–atoms of DME}_{\text{output}})}{(\text{C–atoms of DME}_{\text{input}})} \times 100 \quad (3)$$

$$\text{Product selectivity} = \frac{\text{C–atoms of the product}}{\text{C–atoms of DME}_{\text{input}} - \text{C–atoms of DME}_{\text{output}}} \quad (4)$$

Coke amounts determined via Thermal gravimetric analysis (TGA) measurement and the corresponding GC-MS detection of entrapped hydrocarbon species from spent catalysts TGA was carried out on a Perkin-Elmer Pyris 1 TG analyzer at a heating rate of 10 K min^{-1} from room temperature to 800 °C in air. GC-MS were conducted on Agilent 7890A GC/5975C MSD with HP-5MS column (30 m × 250 μm × 0.25 μm) after flash at 1023 K by PY-2020iD (Frontier Lab).

E. Supplementary Figures and Tables

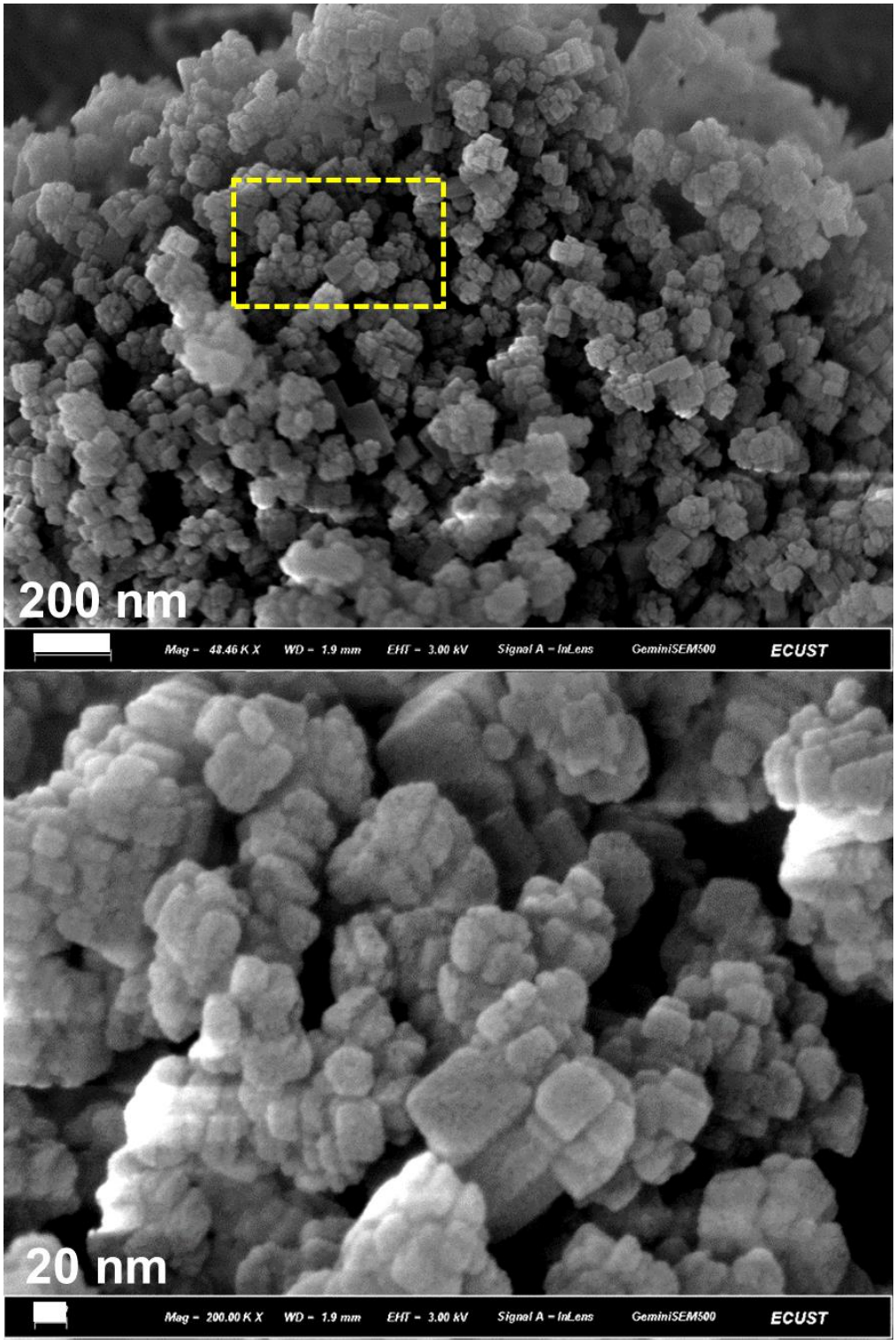

Fig. S1 High magnification FE-SEM images of SAPO-34-N.

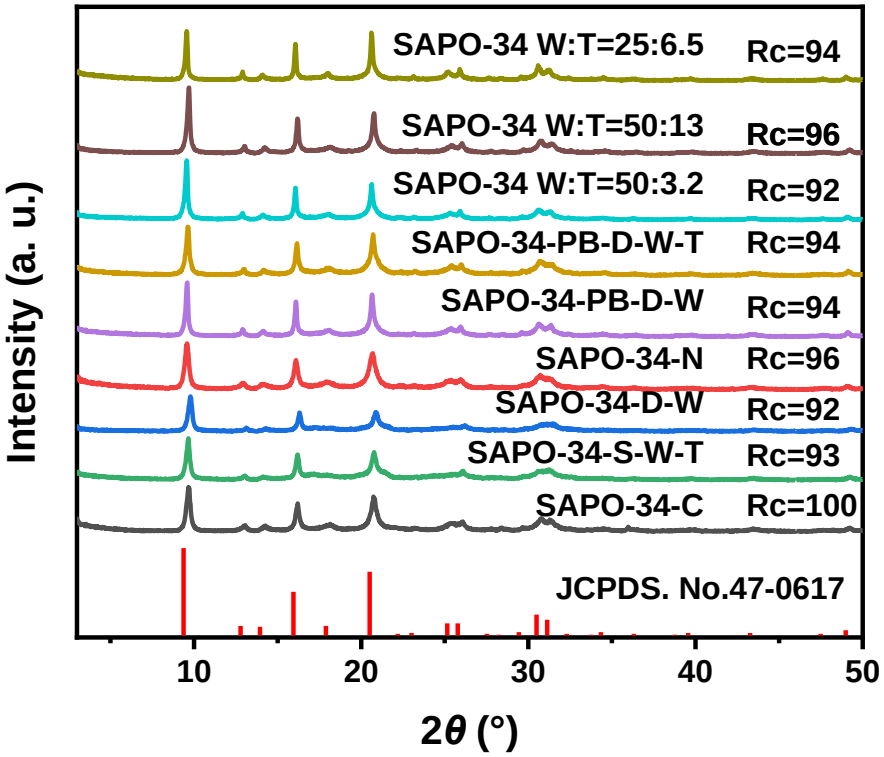

Fig. S2 XRD patterns & relative crystallinity [a] for SAPO-34-C, SAPO-34-S-W-T, SAPO-34-D-W, SAPO-34-N, SAPO-34-PB-D-W, SAPO-34-PB-D-W-T, SAPO-34 W:T=50:3.2 and SAPO-34 W:T=50:13.[b]

[a] Relative crystallinity calculation based on the area of peaks at 2θ = 9.5, 16.0, 20.5, 25.8 and 30.50°, the relative crystallinity of fully crystallized SAPO-34-C.

[b] SAPO-34-N derived from water-toluene biphasic synthesis using AIP as precursor (SAPO-34-N), SAPO-34-C derived from aqueous static crystallization, SAPO-34-D-W derived from aqueous dynamic crystallization, and SAPO-34-S-W-T prepared from water-toluene biphasic media under static crystallization otherwise identical crystallization conditions as that of SAPO-34-N. SAPO-34-PB-D-W derived from aqueous dynamic crystallization using PB as precursor, SAPO-34-PB-D-W-T derived from water-toluene biphasic synthesis; SAPO-34 W:T=50:3.2, 50:13& SAPO-34 W:T=25:6.5 just turn water toluene radio from 50:3.2 , 50:13 to 25:6.5.

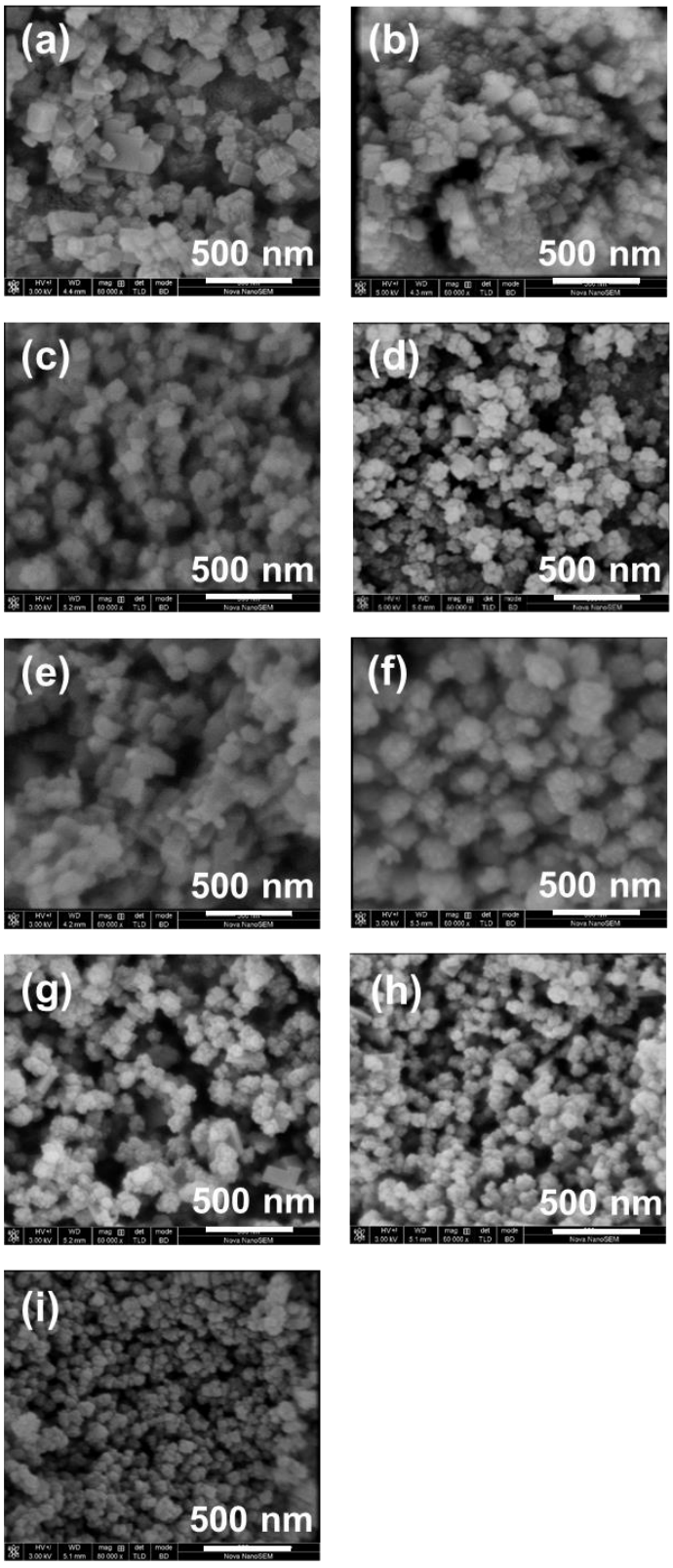

Fig. S3 SEM images of SAPO-34-C (a); SAPO-34-S-W-T (b); SAPO-34-D-W (c); SAPO-34-N (d); SAPO-34-PB-D-W (e); SAPO-34-PB-D-W-T (f); SAPO-34-W:T=50:3.2 (g); SAPO-34-W:T=50:13 (h), SAPO-34-W:T=25:6.5 (i)

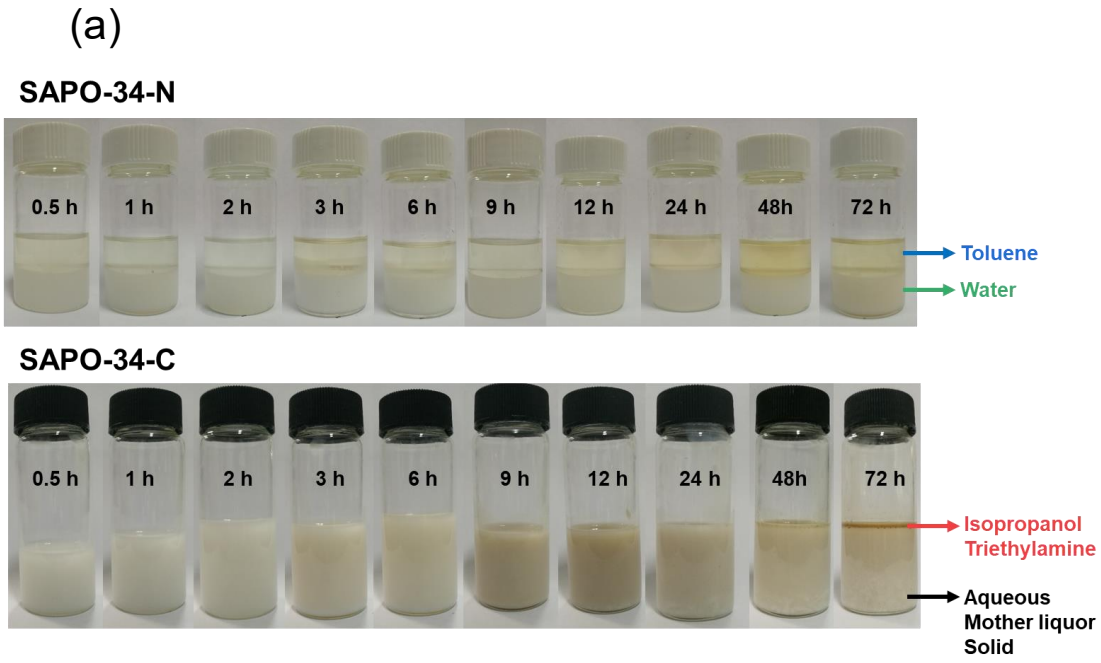

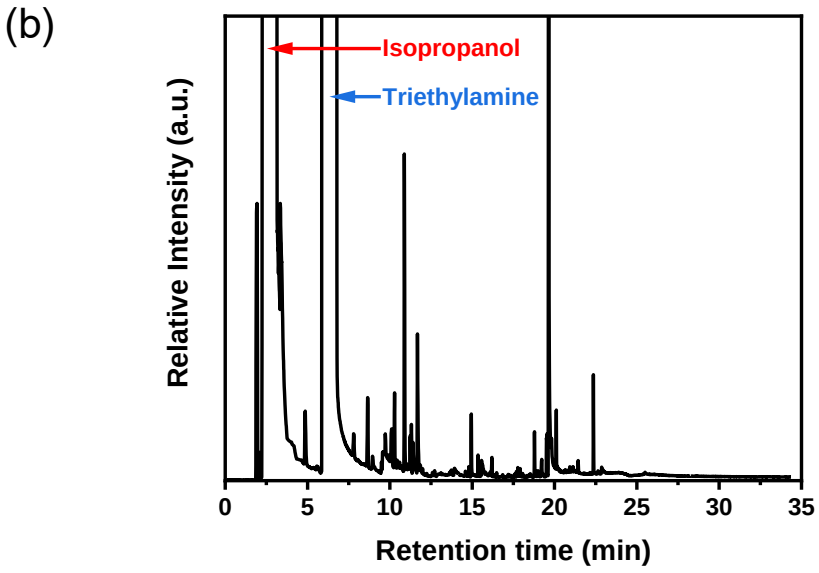

Fig. S4 Photographs of time-dependent products of SAPO-34-N and SAPO-34-C crystallization process (a), and GC-MS of supernatant upper part of mother liquor of SAPO-34-C-72h after centrifugation (b).

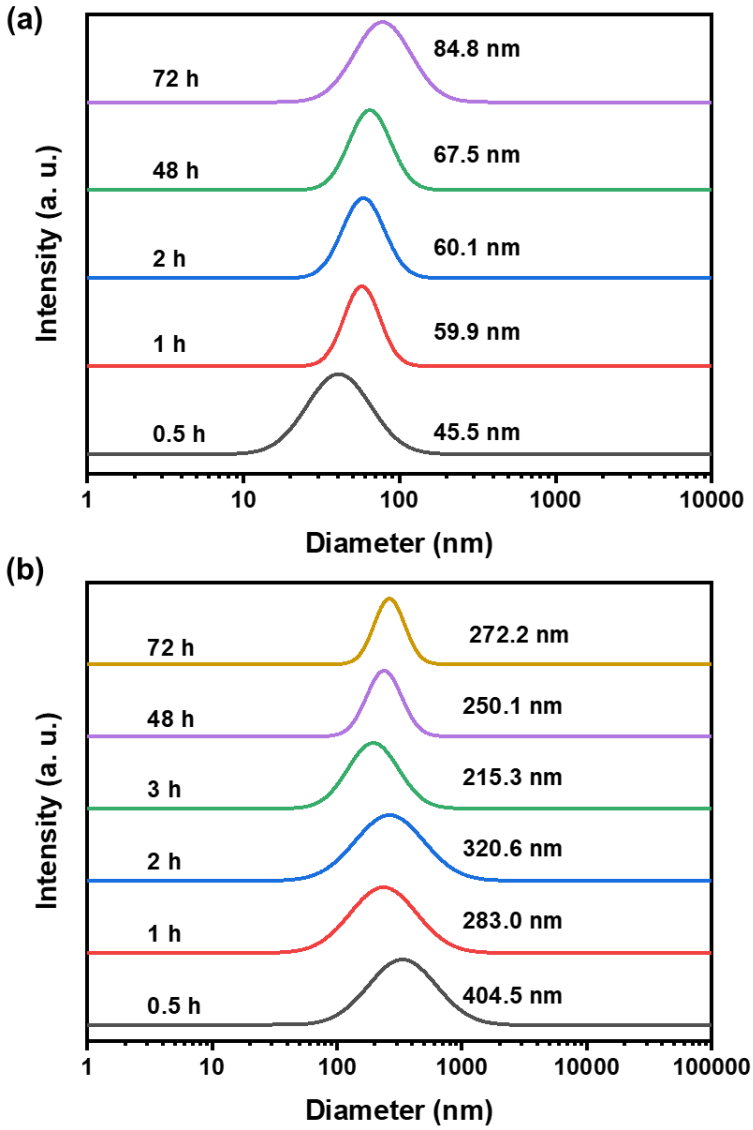

Fig. S5 Dynamic Light Scattering measurements of early stage and final stage of solid dispersion at varied crystallization time for SAPO-34-N (a) and SAPO-34-C (b) formation. [a]

[a] Particle dispersion index of SAPO-34-N-0.5h = 0.211, SAPO-34-N-1h = 0.070, SAPO-34-N-2h = 0.096, SAPO-34-N-48h = 0.091, SAPO-34-N-72h = 0.175, SAPO-34-C-0.5h = 0.391, SAPO-34-C-1h = 0.375, SAPO-34-C-2h = 0.399, SAPO-34-C-2h = 0.218, SAPO-34-C-48h = 0.105, SAPO-34-C-72h = 0.078.

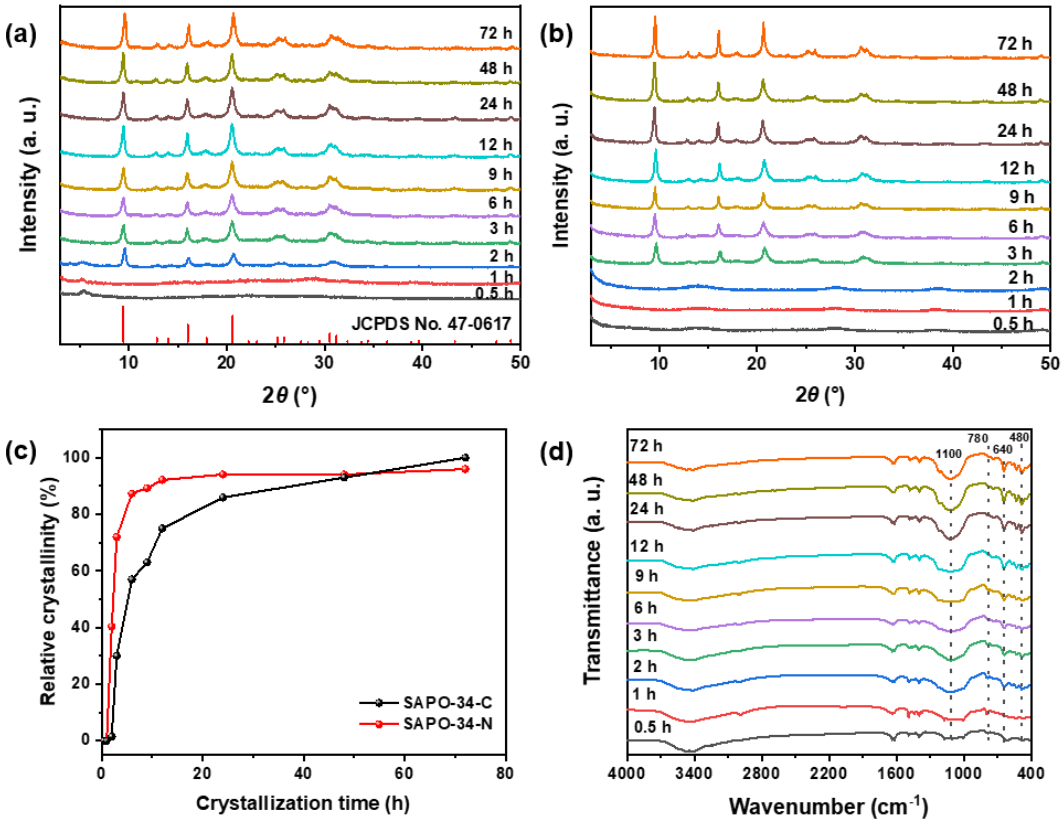

Fig. S6 XRD patterns of the solid products collected at different time points of SAPO-34-N (a), SAPO-34-C (b), relative crystallinity evolution with crystallization time (c)[a], and time-dependent FT-IR of SAPO-34-N (d)[b].

[a] Relative crystallinity calculation based on the area of peaks at 2θ = 9.5, 16.0, 20.5, 25.8 and 30.50 °, the relative crystallinity of fully crystallized SAPO-34-C.

[b] All peaks are assigned as follows: 3650–3000 cm^{-1} arising from the hydroxyl vibration; 1300–1000 cm^{-1} ascribed to the asymmetric stretch of T–O tetrahedra; 740 cm^{-1} due to the symmetric stretch of T–O tetrahedra; the peaks at 640 cm^{-1} corresponding to the vibration of double-6 rings.

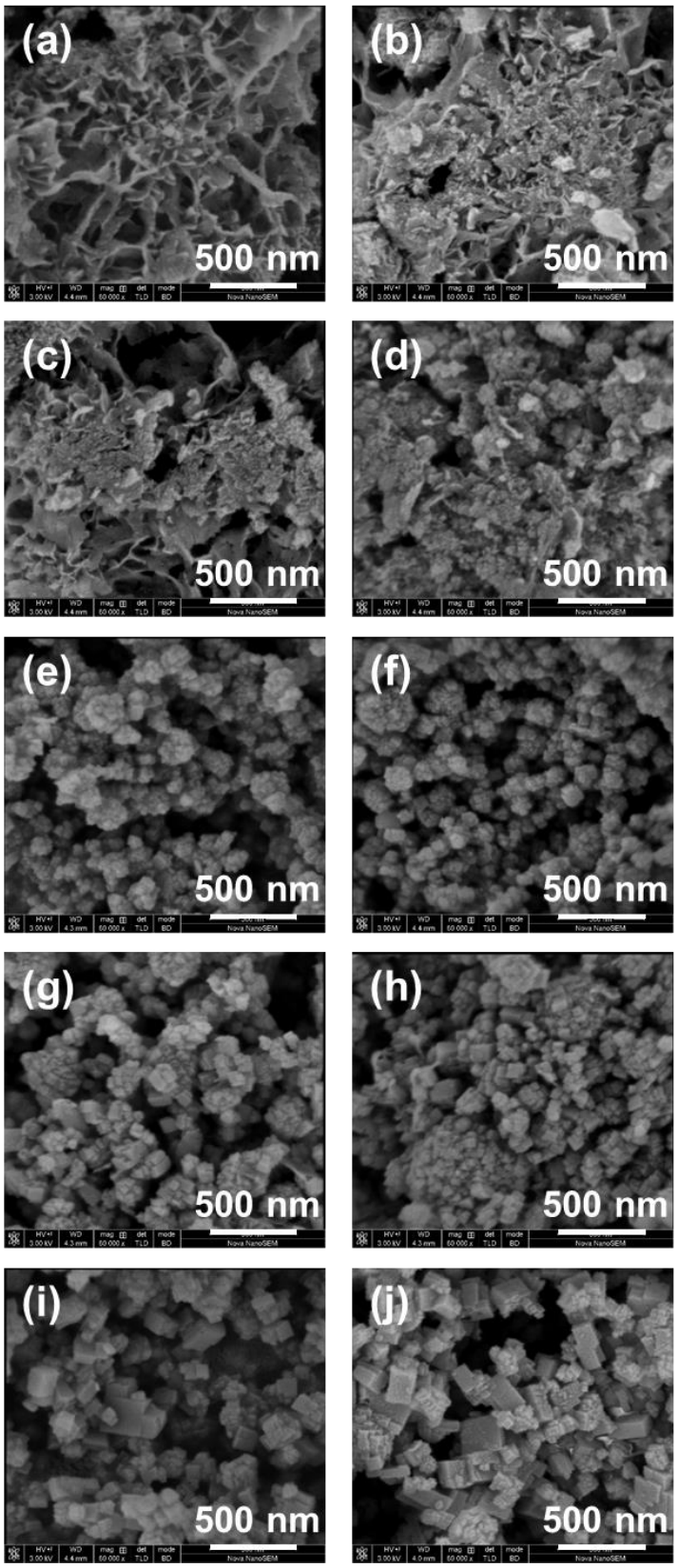

Fig. S7 SEM images of SAPO-34-C-0.5h (a), SAPO-34-C-1h (b), SAPO-34-C-2h (c), SAPO-34-C-3h (d), SAPO-34-C-6h (e), SAPO-34-C-9h (f), SAPO-34-C-12h (g), SAPO-34-C-24h (h), SAPO-34-C-48h (i), SAPO-34-C-72h (j).

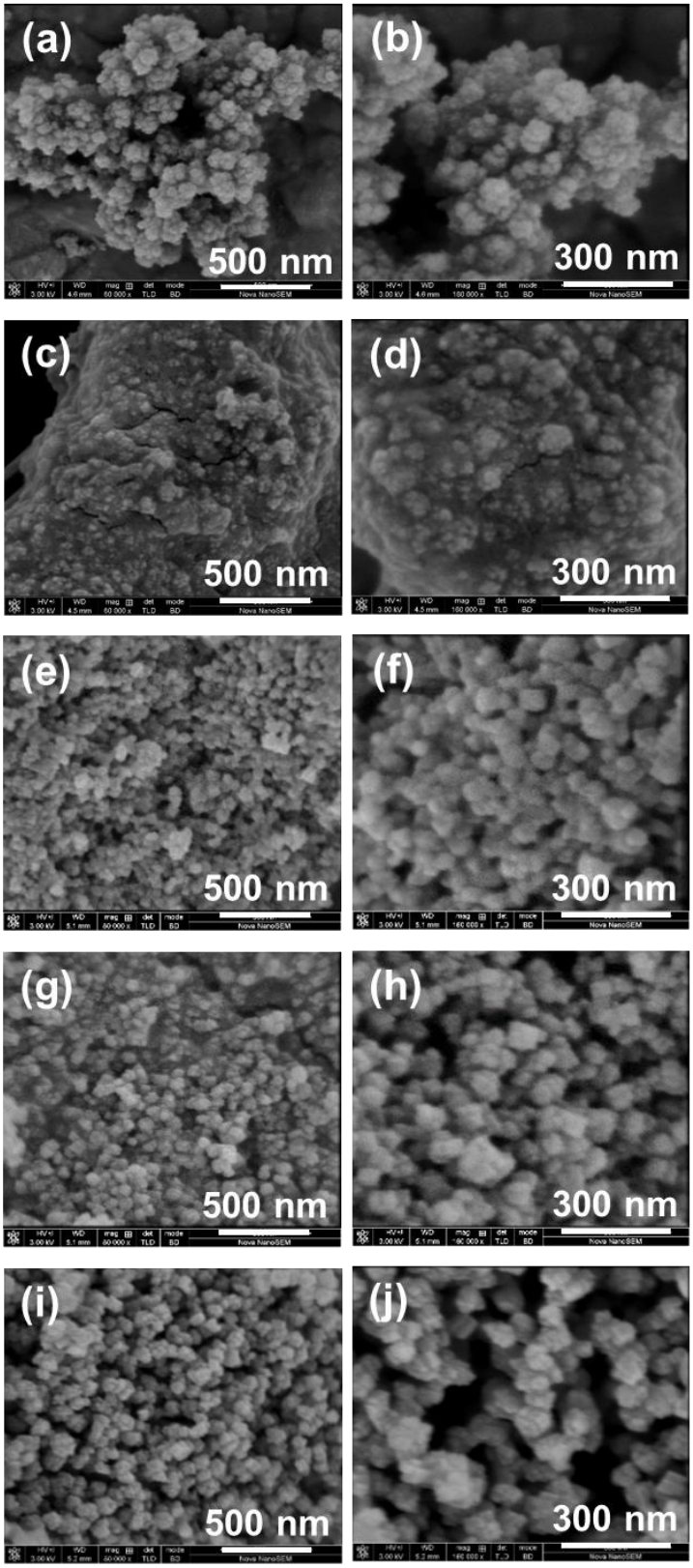

to be continued

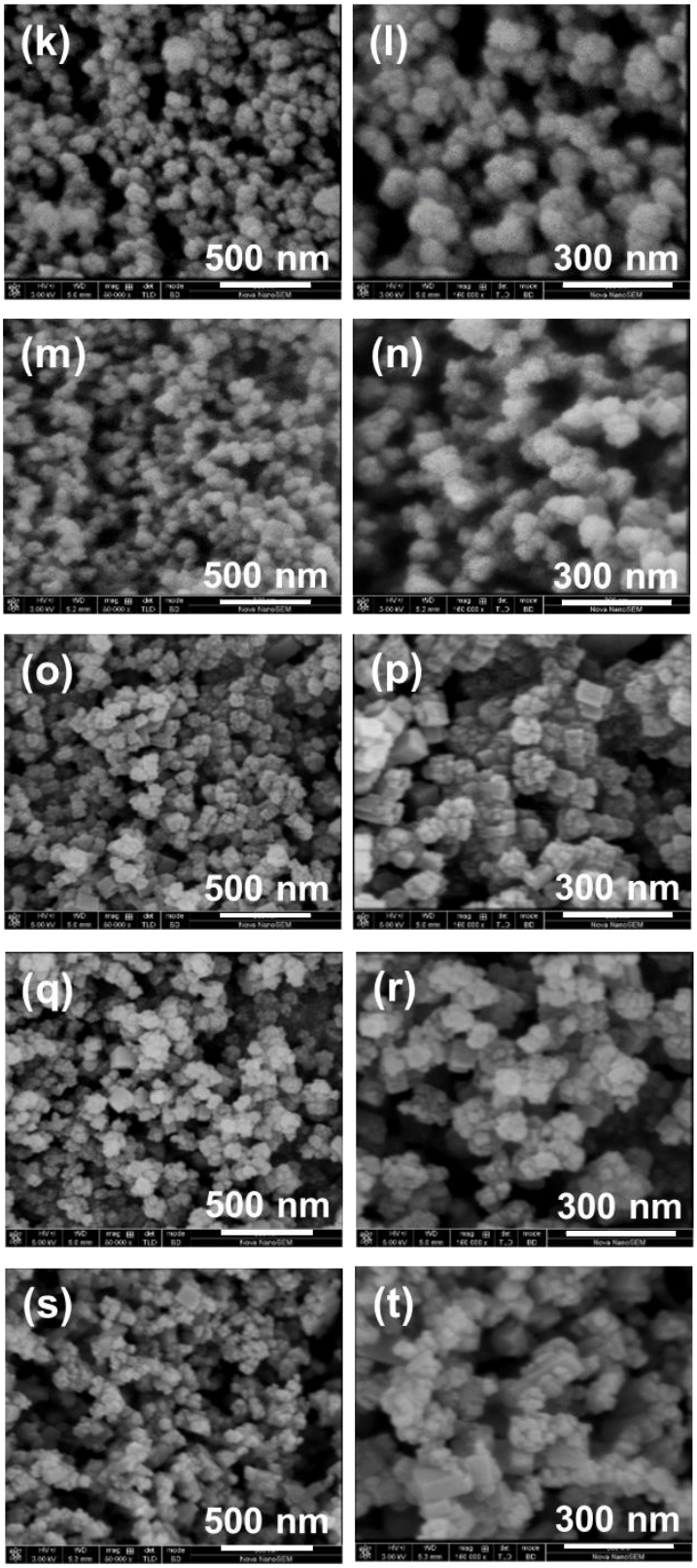

Fig. S8 SEM images of SAPO-34-N-0.5h (a, b), SAPO-34-N-1h (c, d), SAPO-34-N-2h (e, f), SAPO-34-N-3h (g, h), SAPO-34-N-6h (i, j), SAPO-34-N-9h (k, l), SAPO-34-N-12h (m, n), SAPO-34-N-24h (o, p), SAPO-34-N-48h (q, r), SAPO-34-N-72h (s, t).

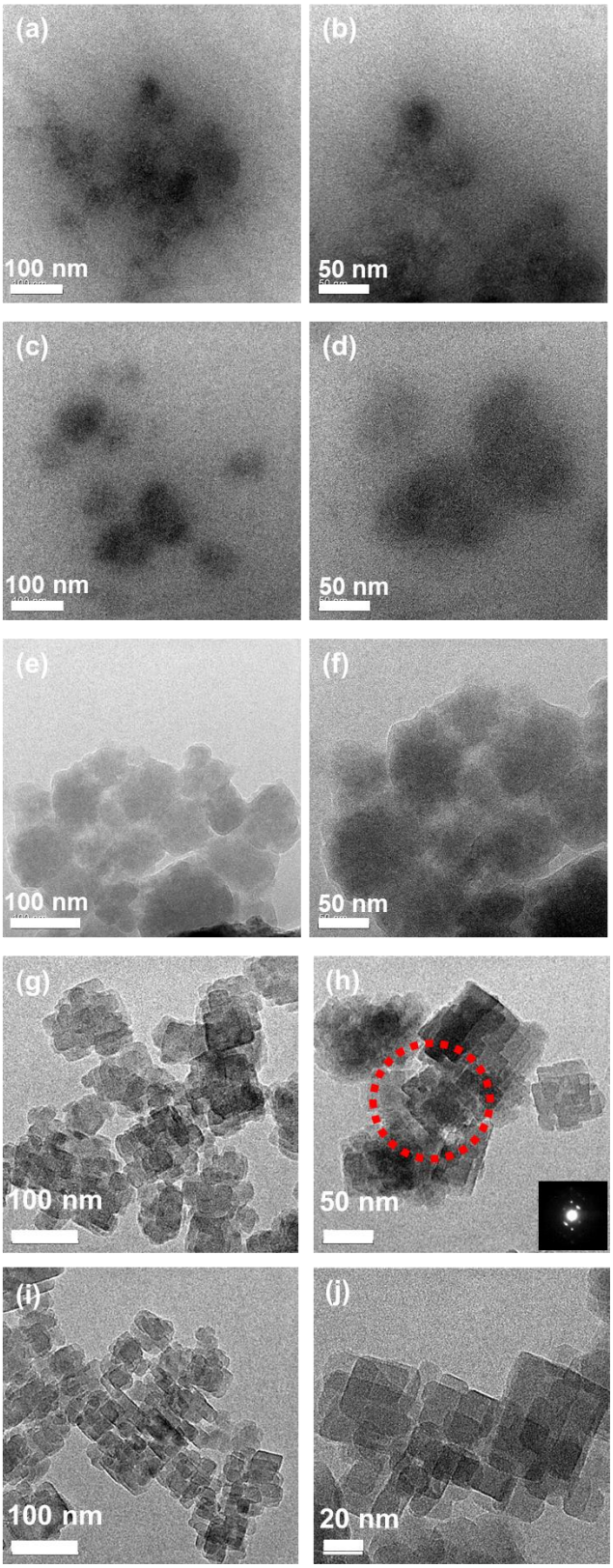

Fig. S9 TEM images of SAPO-34-N-0.5h (a, b), SAPO-34-N-1h (c, d), SAPO-34-N-2h (e, f), SAPO-34-N-24h (g, h), SAPO-34-N-48h (i, j).

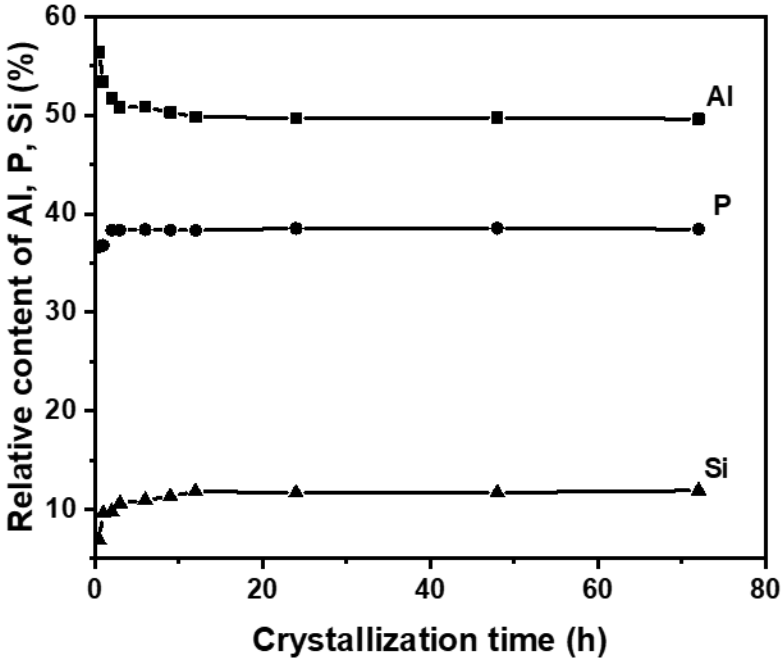

Fig. S10 Chemical composition variations of inorganic components in solid product during crystallization process

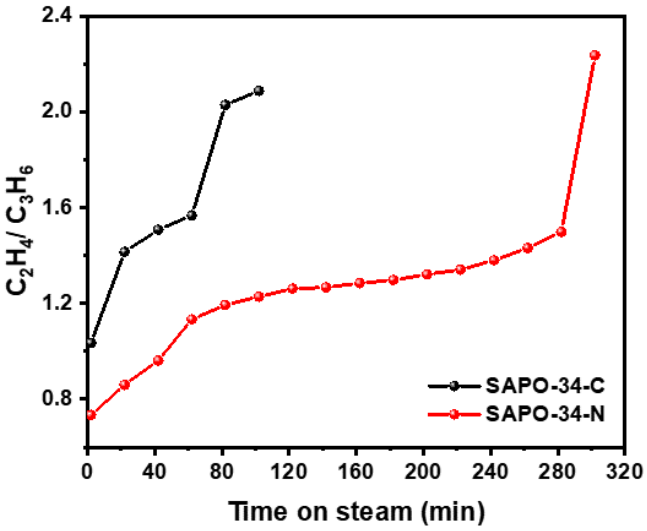

Fig. S11 Time on stream C_2H_4/C_3H_6 of DTO for SAPO-34-N and SAPO-34-C.

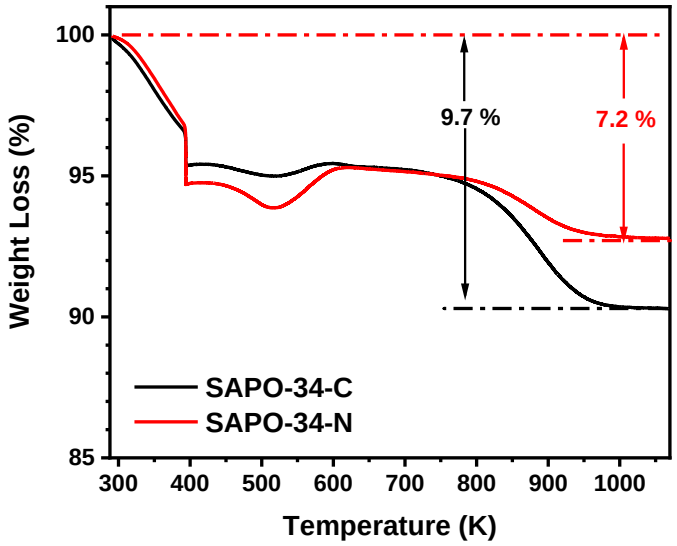

Fig. S12 Coke amounts determined via Thermal gravimetric analysis (TGA) measurement from spent catalysts.

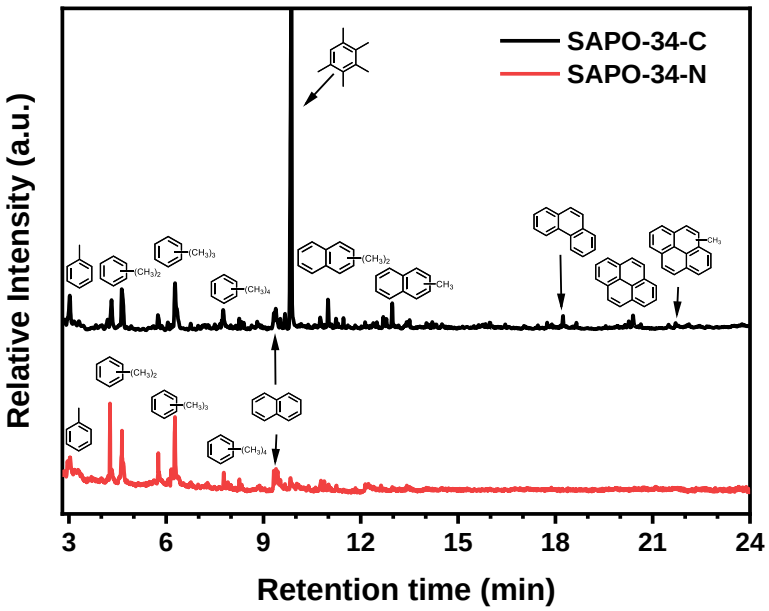

Fig. S13 GC-MS detection of entrapped hydrocarbon species from spent catalysts after DTO reaction.

Table S1 Detailed synthetic procedures of all relevant samples.

Name	Crystallization condition							
	Aluminum source	Static or dynamic	Molar composition					
			Al_2O_3	P_2O_5	SiO_2	TEAOH	H_2O	toluene
SAPO-34-C	AIP	Static	1	1	0.3	2	50	0
SAPO-34-S-W-T	AIP	Static	1	1	0.3	2	50	6.5
SAPO-34-D-W	AIP	Dynamic	1	1	0.3	2	50	0
SAPO-34-N	AIP	Dynamic	1	1	0.3	2	50	6.5
SAPO-34-PB-D-W	PB	Dynamic	1	1	0.3	2	50	0
SAPO-34-PB-D-W-T	PB	Dynamic	1	1	0.3	2	50	6.5
SAPO-34 W:T=50:3.2	AIP	Dynamic	1	1	0.3	2	50	3.2
SAPO-34 W:T=50:13	AIP	Dynamic	1	1	0.3	2	50	13
SAPO-34 W:T=25:6.5	AIP	Dynamic	1	1	0.3	2	25	6.5

Table S2 DTO catalytic results of SAPO-34-C and SAPO-34-N catalysts.

Sample	TOS (min)	Selectivity (%)								
		CH_4	C_2H_4	C_2H_6	C_3H_6	C_3H_8	C_4H_8	C_4H_{10}	C_5^+	$C_2H_4+C_3H_6$
SAPO-34-C	22	1.13	48.05	0.43	33.94	0.63	4.16	6.73	4.88	81.99
SAPO-34-N	102	1.19	46.09	0.65	40.65	0.44	2.61	5.06	3.27	86.75